

# Supporting Information

## Surface-Facet-Dependent Phonon Deformation Potential in Individual Strained Topological Insulator $\text{Bi}_2\text{Se}_3$ Nanoribbons

Yuan Yan,<sup>§,†,\*</sup> Xu Zhou,<sup>#,±,†</sup> Han Jin,<sup>#,†</sup> Cai-Zhen Li,<sup>#</sup> Xiaoxing Ke,<sup>Δ</sup> Gustaaf Van  
Tendeloo,<sup>Δ</sup> Kaihui Liu,<sup>#,‡,±</sup> Dapeng Yu,<sup>#,‡,±</sup> Martin Dressel,<sup>§</sup> and Zhi-Min Liao<sup>#,‡,\*</sup>

<sup>§</sup>1. Physikalisches Institut, Universität Stuttgart, 70550 Stuttgart, Germany,

<sup>#</sup>State Key Laboratory for Mesoscopic Physics, Department of Physics, Peking University, 100871  
Beijing, China,

<sup>±</sup>Academy for Advanced Interdisciplinary Studies, Peking University, 100871 Beijing, China,

<sup>Δ</sup>EMAT (Electron Microscopy for Materials Science), University of Antwerp, Groenenborgerlaan 171,  
B-2020 Antwerp, Belgium,

<sup>‡</sup>Collaborative Innovation Center of Quantum Matter, Beijing, China

<sup>†</sup>These authors contributed equally to this work

<sup>\*</sup>Address correspondence to [yuan.yan@pi1.physik.uni-stuttgart.de](mailto:yuan.yan@pi1.physik.uni-stuttgart.de); [liaozm@pku.edu.cn](mailto:liaozm@pku.edu.cn)

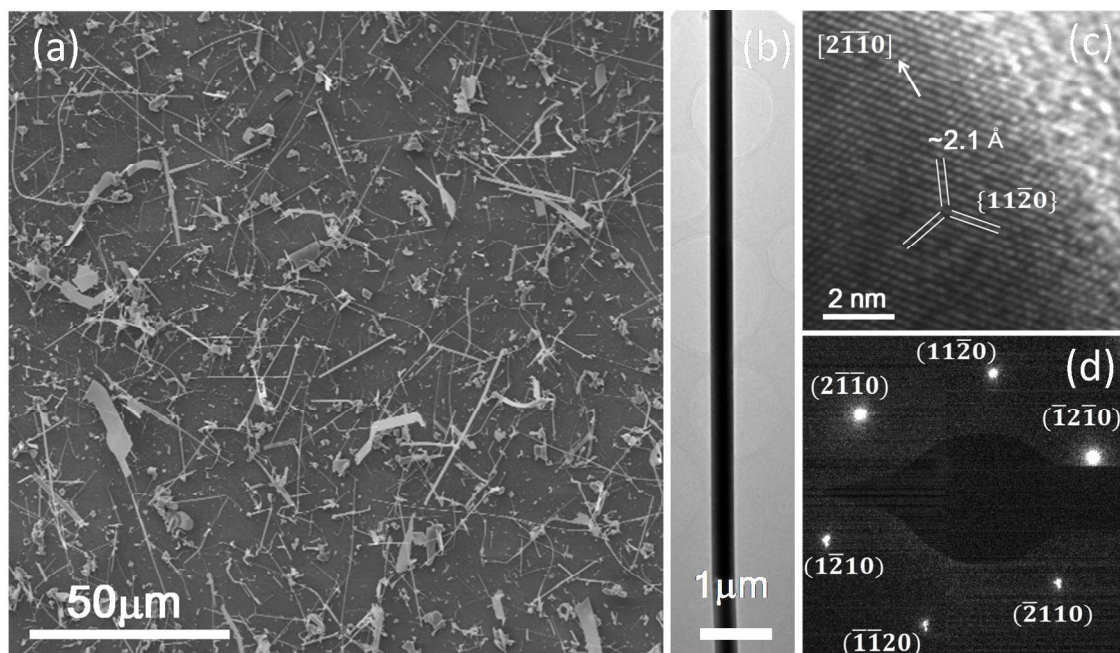


**Figure S1.** Characterization of as-grown  $\text{Bi}_2\text{Se}_3$  nanoribbons. (a) SEM, (b) TEM, (c) HRTEM images and (d) SAED pattern of as grown  $\text{Bi}_2\text{Se}_3$  nanoribbons.

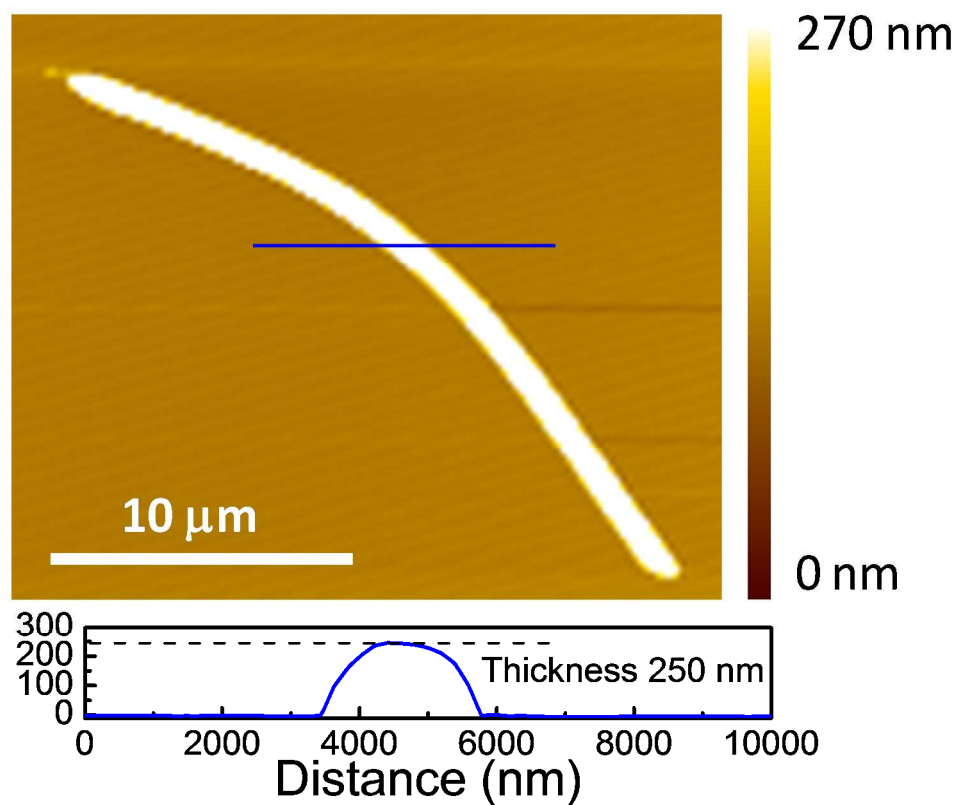


**Figure S2.** Atomic force microscopy (AFM) characterization of a representative  $\text{Bi}_2\text{Se}_3$  nanoribbon after Raman measurements. The thickness is 250 nm.

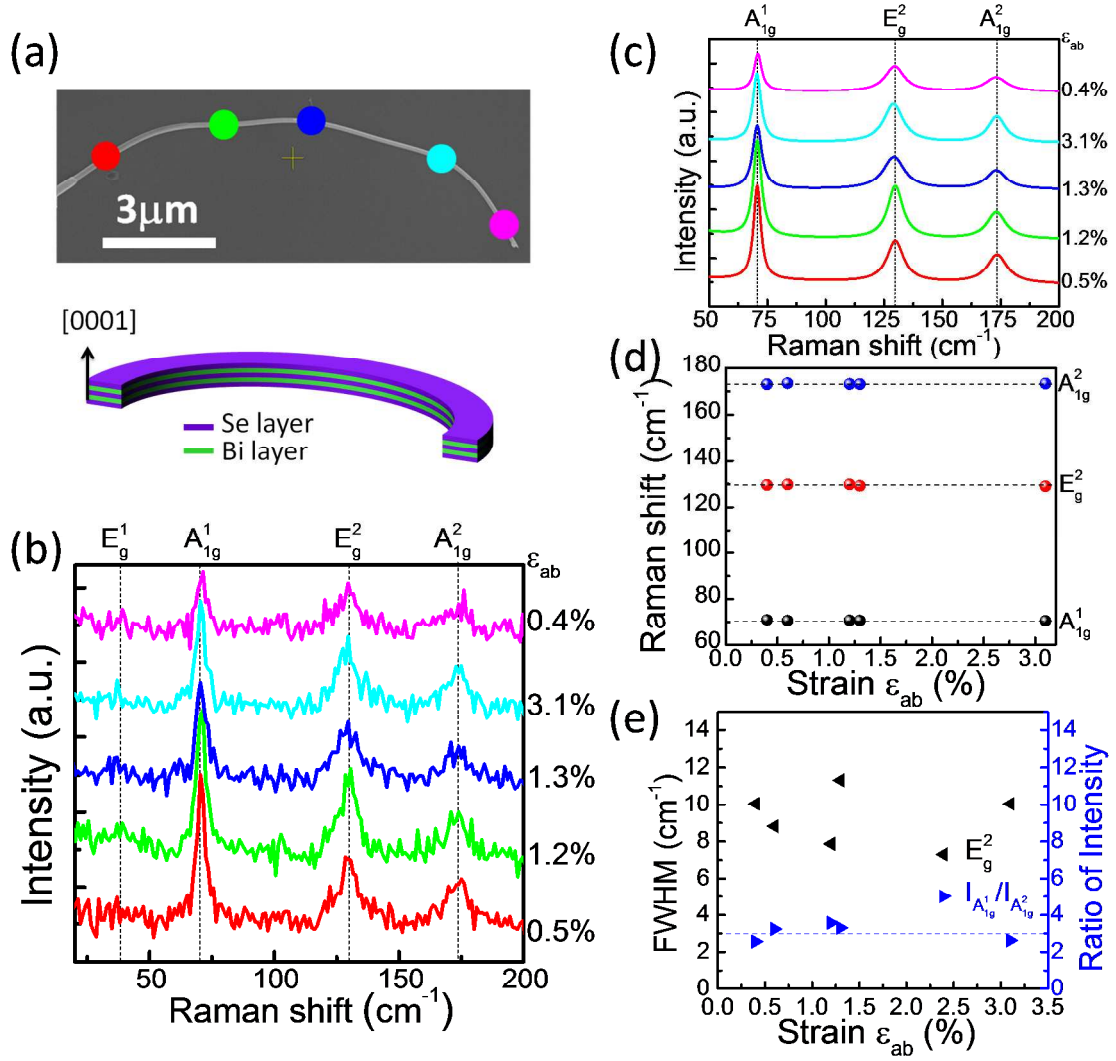


**Figure S3.** Raman spectra of a strained  $\text{Bi}_2\text{Se}_3$  nanoribbon with the  $\{0001\}$  surface parallel to the substrate plane. (a) SEM image and schematic illustration of a bent  $\text{Bi}_2\text{Se}_3$  nanoribbon with a width of 145 nm and a thickness of 130 nm. (b) Raman spectra and (c) Lorentzian fitted Raman spectra collected at different positions along the  $\text{Bi}_2\text{Se}_3$  nanoribbon. The colored curves correspond to five different positions on the  $\text{Bi}_2\text{Se}_3$  nanoribbon. Frequencies of the vibrational modes are indicated by dashed lines. (d) Raman shift of the vibrational modes ( $A_{1g}^1$ ,  $E_g^2$ ,  $A_{1g}^2$ ) versus strain. (e) FWHM of  $E_g^2$  mode and ratio of intensities  $I_{A_{1g}^1}/I_{A_{1g}^2}$  as a function of strain.

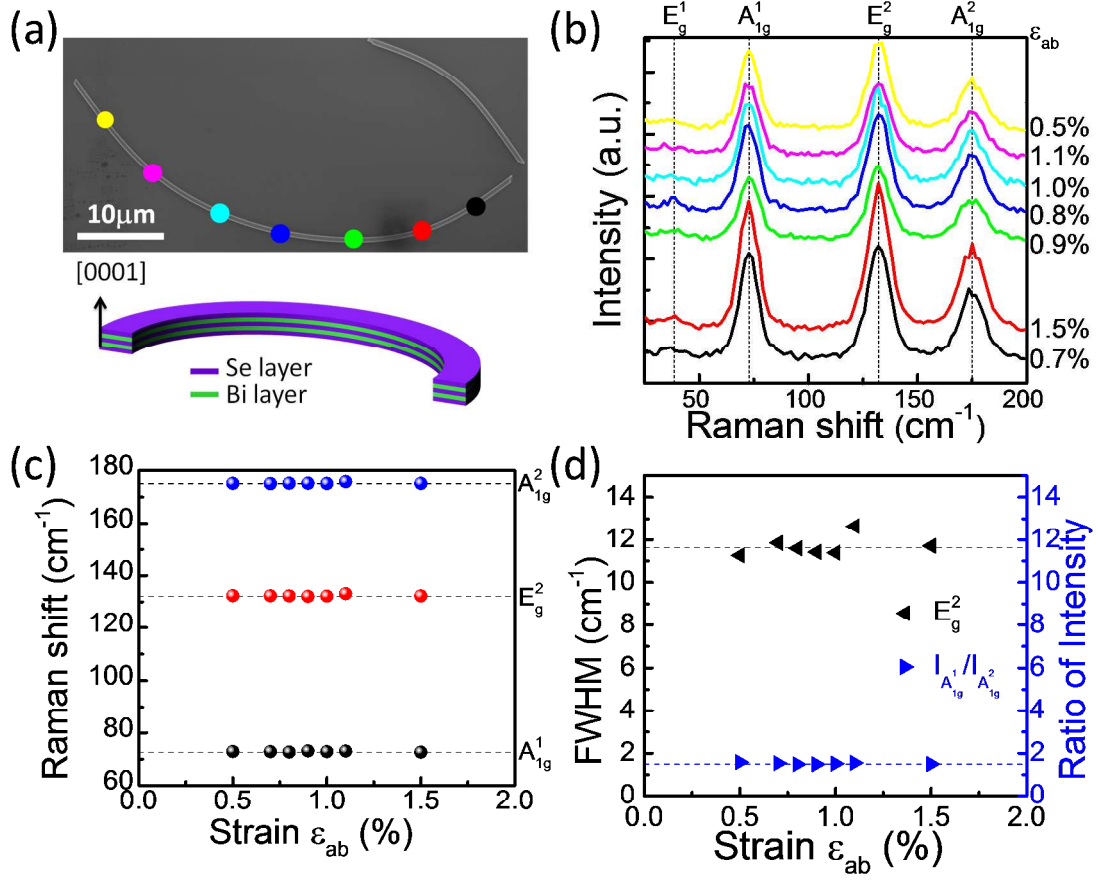


**Figure S4.** Raman spectra of a strained  $\text{Bi}_2\text{Se}_3$  nanoribbon with the  $\{0001\}$  surface parallel to the substrate plane. (a) SEM image and schematic illustration of a bent  $\text{Bi}_2\text{Se}_3$  nanoribbon with a width of 320 nm and a thickness of 250 nm. (b) Raman spectra collected at different positions along the  $\text{Bi}_2\text{Se}_3$  nanoribbon. The color of each curve corresponds to seven different points on the  $\text{Bi}_2\text{Se}_3$  nanoribbon. Frequencies of each vibrational mode are indicated by dashed lines. (c) Raman shift of the vibrational modes ( $A_{1g}^1$ ,  $E_g^2$ ,  $A_{1g}^2$ ) versus strain. (d) FWHM of  $E_g^2$  mode and ratio of intensities  $I_{A_{1g}^1}/I_{A_{1g}^2}$  as a function of strain.

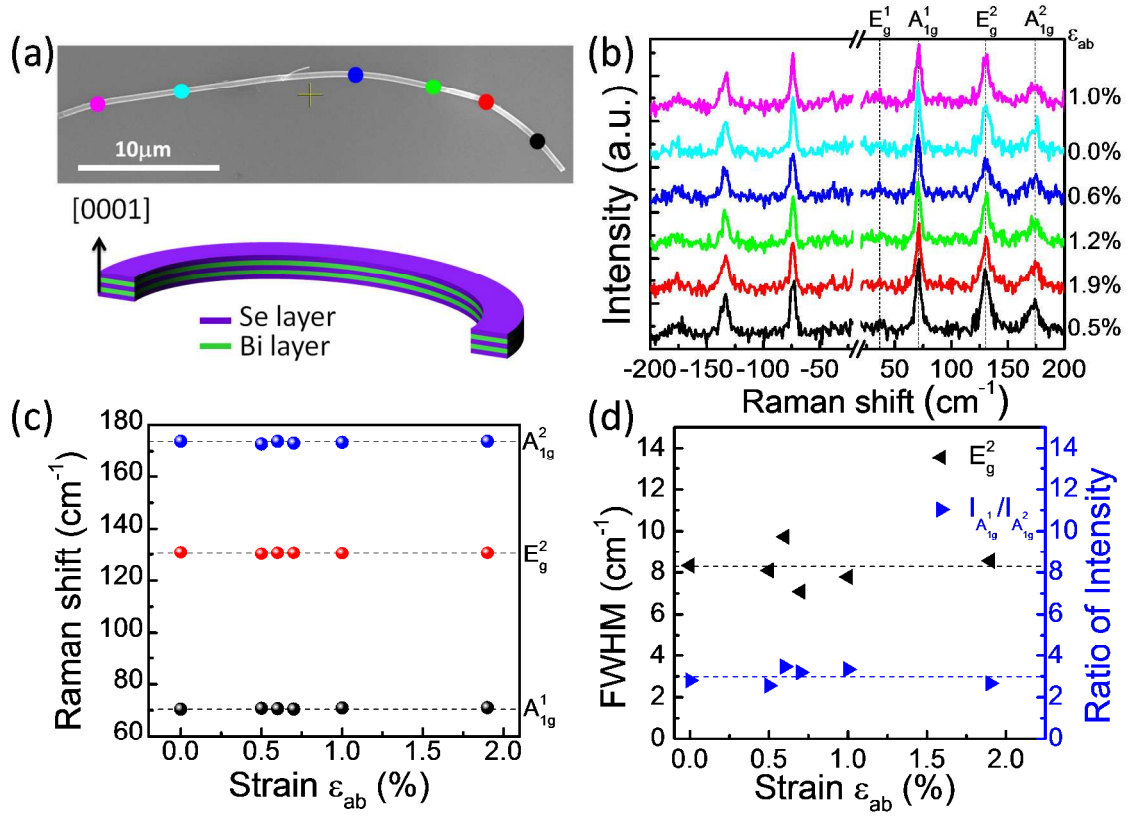


**Figure S5.** Raman spectra of a strained  $\text{Bi}_2\text{Se}_3$  nanoribbon with the  $\{0001\}$  surface parallel to the substrate plane. (a) SEM image and schematic illustration of a bent  $\text{Bi}_2\text{Se}_3$  nanoribbon with a width of 425 nm and a thickness of 170 nm. (b) Raman spectra collected at the different positions along the  $\text{Bi}_2\text{Se}_3$  nanoribbon. The color of each curve corresponds to six different points on the  $\text{Bi}_2\text{Se}_3$  nanoribbon. Frequencies of each vibrational mode are indicated by dashed lines. (c) Raman shift of the vibrational modes ( $A_{1g}^1$ ,  $E_g^2$ ,  $A_{1g}^2$ ) versus strain. (d) FWHM of  $E_g^2$  mode and ratio of intensities  $I_{A_{1g}^1}/I_{A_{1g}^2}$  as a function of strain.

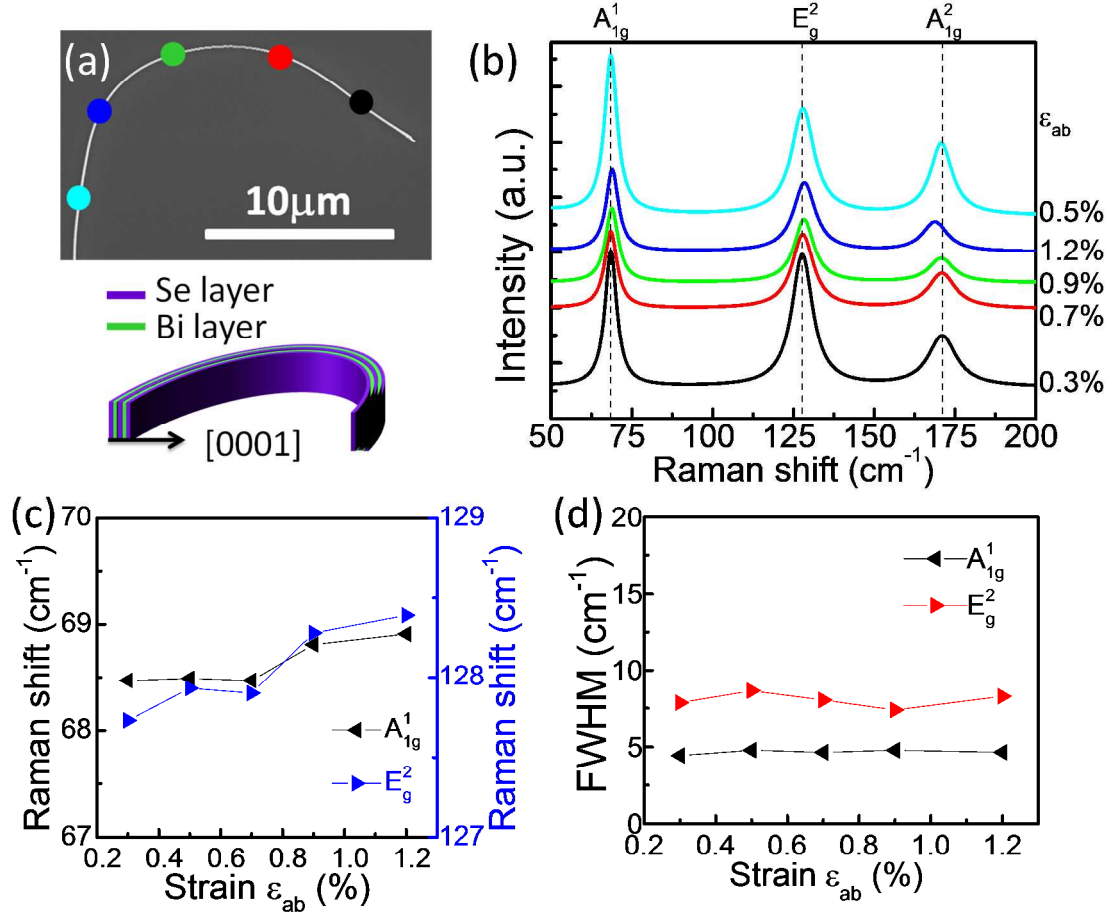


**Figure S6.** Raman spectra of a strained  $\text{Bi}_2\text{Se}_3$  nanoribbon with the  $\{0001\}$  surface perpendicular to the substrate plane and the exposed  $\{01\bar{1}5\}$  top surface. (a) SEM image and schematic illustration of a bent  $\text{Bi}_2\text{Se}_3$  nanoribbon with a thickness of 120 nm. (b) Lorentzian fitted Raman spectra collected at the different positions along the  $\text{Bi}_2\text{Se}_3$  nanoribbon. The color of each curve corresponds to five different points on the  $\text{Bi}_2\text{Se}_3$  nanoribbon. (c) Raman shift and (d) FWHM of  $A_{1g}^1$  and  $E_g^2$  modes *versus* strain.

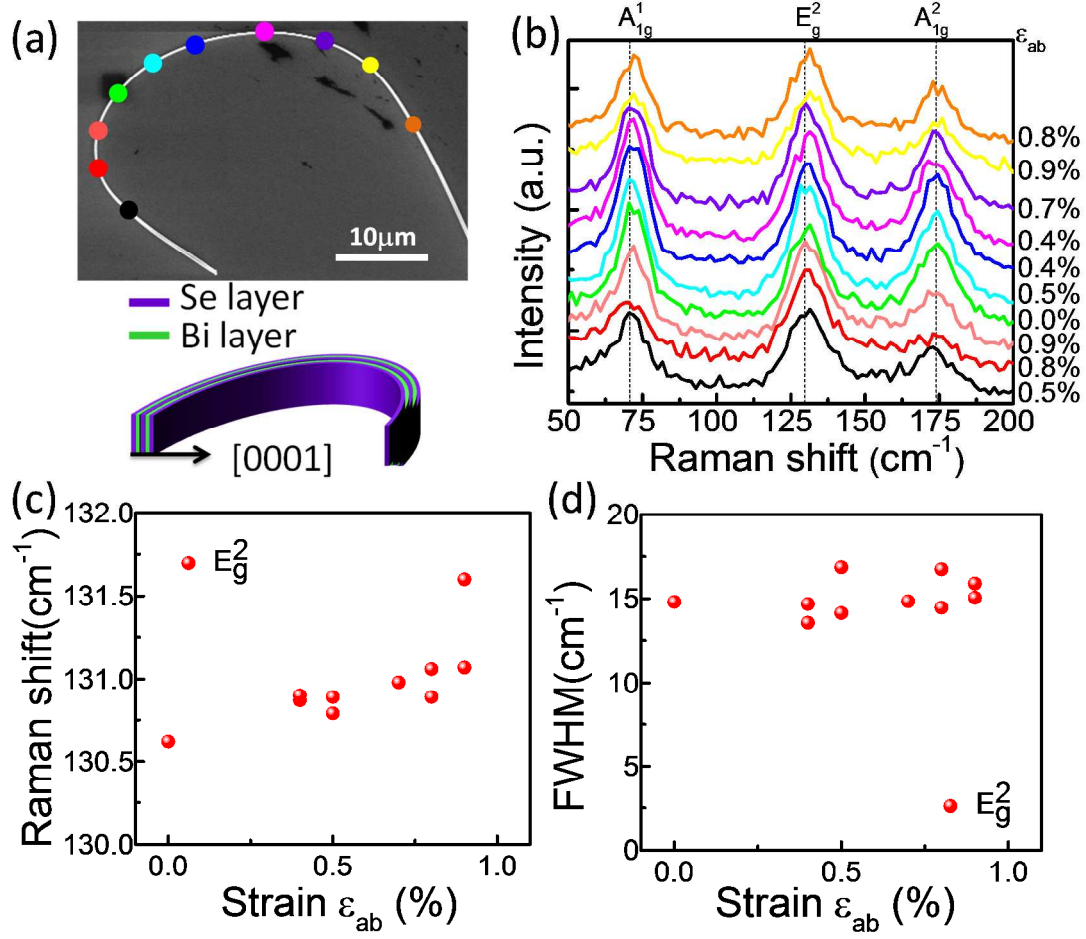


**Figure S7.** Raman spectra of a strained  $\text{Bi}_2\text{Se}_3$  nanoribbon with the  $\{0001\}$  surface perpendicular to the substrate plane and the exposed  $\{01\bar{1}5\}$  top surface. (a) SEM image and schematic illustration of a bent  $\text{Bi}_2\text{Se}_3$  nanoribbon with a thickness of 190 nm. (b) Raw Raman spectra collected at the different positions along the  $\text{Bi}_2\text{Se}_3$  nanoribbon. The color of each curve corresponds to ten different points on the  $\text{Bi}_2\text{Se}_3$  nanoribbon. (c) Raman shift and (d) FWHM of  $E_g^2$  mode *versus* strain.